CHARACTERISTIC PREDICTIONS OF TOPOLOGICAL SOLITON MODELS

V. B. Kopeliovich [*]

Institute for Nuclear Research, Russian Academy of Sciences
117312, Moscow, Russia

Characteristic predictions of chiral soliton models (the Skyrme model and its extentions) are discussed. The chiral soliton model predictions of low-lying dibaryon states qualitatively agree with the recent evidence for the existence of narrow dibaryons in reactions of the inelastic proton scattering on deuterons and the double photon radiation $pp \to pp\gamma\gamma$. The connection between magnetic moment operators and inertia tensors valid for arbitrary $SU(2)$ skyrmion configurations allows us to estimate the electromagnetic decay width of some states of interest. Predictions of a different type are multibaryons with a nontrivial flavor (strangeness, charm or bottom), which can be found, in particular, in high-energy heavy ions collisions. It is shown that the large-B multiskyrmions given by the rational map ansatze can be described within the domain-wall approximation or as a spherical bag with the energy and the baryon number density concentrated at its boundary.

PACS: 12.39.Dc, 13.75.Cs, 14.65.-q

1. INTRODUCTION

The chiral soliton approach provides a very economical method of describing baryonic systems with different baryon numbers, starting with several basic concepts and ingredients incorporated in the model Lagrangian [1, 2]. The latter is the truncated Lagrangian of effective field theories widely used in describing the low-energy meson and baryon interactions [3]. Within this approach, baryons or baryonic systems appear as quantized solitonic solutions of the equations of motion characterized by the so-called winding number or topological charge. If the concept of topological soliton models is accepted and the baryons are indeed skyrmions, it is clear why isospin exists in Nature: the number 3 of the $SU(2)$ isospin group generators coincides with the number of space dimensions, thereby allowing a correlation between $SU(2)$ chiral fields and space coordinates resulting in the appearence of topological solitons.

It has been found numerically that the lowest-energy chiral field configurations possess different topological properties — the shape of the mass and B-number distribution — for different values of B. A

sphere occurs for the $B = 1$ hedgehog [1], a torus for $B = 2$ [4], a tetrahedron for $B = 3$, a cube for $B = 4$ [5], and higher polyhedrons for greater baryon numbers [5–7]. A paradoxical feature of the approach is that the baryon/nucleon individuality is absent in the lowest-energy static configurations (we note that any of the known lowest-energy configurations can be made of a number of slightly deformed tori). It is believed that the standard picture of nuclei must emerge when the motion due to nonzero modes (vibration and breathing) is taken into account. Finding the relative position of states with different quantum numbers (spin, isospin, flavor, $SU(3)$ representation, etc.) requires calculating the zero-mode quantum corrections to the energy of a baryonic system. Corrections of this type were first calculated for configurations of the «hedgehog» type [8] and later, for axially symmetric configurations [9, 10] and for more general configurations for the $SU(2)$ [11] and $SU(3)$ symmetry groups [12, 13].

The chiral soliton approach provides the concept of nuclear matter that is different from the commonly accepted assumption that the nuclear matter is constructed from separate nucleons only. To find the «smoking gun» for this unusual concept, it is necessary to find some states that cannot be made of separate nucleons, e.g., because of the Pauli exclusion princi-

[*]E-mail: kopelio@al20.inr.troitsk.ru

ple. The simplest possibility is to consider the $B = 2$ system, where the Pauli principle strictly and unambiguosly forbids definite sets of quantum numbers for the system consisting of separate nucleons.

In this paper, we first discuss the $SU(2)$ case (Sec. 2), where supernarrow low-lying dibaryons were predicted [14], and estimate their electromagnetic decay width. We next consider the $SU(3)$ extention of the chiral soliton model and extend the previous estimates of the spectra of multibaryons with flavor (strangeness, charm or bottom quantum number) to higher baryon numbers, where the necessary theoretical information on multiskyrmions is available [7]. A simplified model for large-B multiskyrmions given by rational maps (RM) [15] is presented that allows us to establish the relation to the domain-wall or bag approximation (Sec. 4). The technical details required for calculations are available in the literature; some of them are given in the Appendices, where several statements valid for any chiral soliton are proved and useful expressions for the $SU(2)$ skyrmion inertia tensors (still lacking in the literature) are presented.

2. NARROW DIBARYONS BELOW THE $NN\pi$ THRESHOLD

The topological chiral solitons (skyrmions) are classical configurations of chiral fields incorporated in a unitary matrix $U \in SU(2)$ or $SU(3)$ and characterized by the topological, or winding number identified with the baryon number B. The classical energy (mass) of these configurations M_{cl} is usually found by minimizing the energy functional that depends on chiral fields. As any extended object, skyrmions also possess other characteristics, e.g., inertia moments Θ (inertia tensors in the general case, see Appendix A), mean square radii of the mass and baryon number distribution, etc. The quantization of the zero modes of chiral solitons allows obtaining the spectrum of states with different values of quantum numbers: spin, isospin, strangeness, etc. [8–13]. Because this approach leads to a reasonable description of various properties of baryons, nucleons, and hyperons, it is interesting to consider predictions of the models of this type for baryonic systems with $B \geq 2$. The energy of $SU(2)$ quantized states with the axial symmetry can be written as [9, 10]

$$E = M_{cl} + \frac{I(I+1)}{2\Theta_I} + \frac{J(J+1)}{2\Theta_J} + $$
$$+ \frac{(J_3^{bf})^2}{2B^2\Theta_3}\left(1 - \frac{\Theta_3}{\Theta_I} - B^2\frac{\Theta_3}{\Theta_J}\right), \quad (1)$$

where I and J are the isospin and the spin of the system, J_3 is the body-fixed third (or z) component of the angular momentum, which can be considered as an additional internal quantum number of the system, and $B = n$ is the azimuthal winding number for the lowest-energy axially symmetric configurations. This formula, rigorously obtained from a model Lagrangian [9, 10], has a very transparent physical interpretation. The technical details involving the known Lagrangian of the Skyrme model, expressions for M_{cl}, inertia tensors, and some other formulas can be found in Appendix A.

The (generalized) axial symmetry of the configuration with $B = 2$ leads to a certain constraint on the body-fixed third components of the isospin and the angular momentum:

$$J_3^{bf} = -nI_3^{bf} = -nL$$

(see [9, 10]). For the states with $I = 1$ and $J = 0$, or $I = 0$ and $J = 1$, and also $I = J = 1$, it then follows that

$$I_3^{bf} = J_3^{bf} = L = 0.$$

Therefore, the last term in (1), which is proportional to $J_3^{bf\,2}$, is absent in these cases. Because the parity of the configuration is equal to $P = (-1)^L$ [10], all the above states have a positive parity. For the state with $I = 0$ and $J = 2$, we can also have

$$I_3^{bf} = J_3^{bf} = 0,$$

as well as

$$I_3^{bf} = L = 1, \quad J_3^{bf} = -2.$$

At large B, it can also be shown (see Appendix A) that only the first two terms in (1), those proportional to $I(I+1)$ and $J(J+1)$, are important in the quantum correction to the energy.

It was noted a long time ago [9] that the quantum correction for the deuteron-like state with $I = 0$, $J = 1$, given by $E_d^{rot} = 1/\Theta_J(B = 2)$ is by approximately 30 MeV smaller than the correction for the «quasi-deuteron» state with $I = 1$, $J = 0$ given by $E_{d'}^{rot} = 1/\Theta_I(B = 2)$. This occurs for all the known versions of the model, without any tuning of the parameters, and can therefore be considered as an intrinsic property of the chiral soliton models originating from effective field theories. Further investigations of nonzero modes of the two-nucleon system have shown that with many (albeit not all) of them taken into account, the binding energy of the deuteron can be reduced to $\sim$ 6 MeV [16] if it is considered as a difference between states with the deuteron and the quasideuteron quantum numbers. As previously, we

here consider the differences of the quantized state energies because they are free of many uncertainties, e.g., those due to unknown loop corrections to the masses of skyrmions (see [17, 18] and discussions below).

In accordance with Eq. (1), some dibaryons are predicted to be decoupled from the 2-nucleon channel as a consequence of the Pauli principle [14]. For example, there is a prediction for the state with the isospin $I = J = 1$, positive parity, and the energy below the threshold for the decay into $NN\pi$ with

$$E_D^{rot} = 1/\Theta_J(B = 2) + 1/\Theta_I(B = 2).$$

This dibaryon cannot be seen in nucleon–nucleon interactions directly, but can be observed in the reaction $NN \to NN\gamma\gamma$, where one photon is required to produce D and the second appears from the decay of D, e.g.,

$$pp \to D^{++}\gamma \to pp\gamma\gamma.$$

The chiral soliton models predict the state D with the isospin $I = J = 1$ at the energy about 50–60 MeV above the NN threshold [14].

In [10], it was shown that the states for which the sum $I + J$ is even (0, 2, etc.) and the parity is positive are forbidden by constraints of the Finkelstein–Rubinstein type arising as a consequence of the requirement that the configuration can be presented as a system of two unit hedgehogs at large relative distances such that these unit skyrmions possess fermionic properties. This implies that the configurations that cannot be considered as consisting of two nucleons were ignored in [10]. In [14], on the contrary, we abandoned this requirement. We also note that the state with $I = 0$, $J = 2$, which was forbidden in [10], can in fact be the $^3D_2$ state of two nucleons and should not be forbidden by the FR constraint. This particular case must therefore be analyzed more carefully.

It is possible to estimate the width of the radiative decay $D \to NN\gamma$. Electromagnetic nucleon formfactors can be described sufficiently well within the Skyrme soliton model in a wide interval of momentum transfers [19]. A reasonable agreement with the data takes place for the deuteron and $2N$ systems [10], and therefore, one can expect reasonable predictions for systems with greater baryon numbers or with unusual properties. The dimensional estimate of the narrow dibaryon decay width was made in [14] providing the lower bound for the decay width given by several eV. To make a more realistic estimate, one can consider a transition of the magnetic type, $D \to NN\gamma$ or $d\gamma$. The amplitude of the direct process due to the magnetic dipole transition can be written as

$$M_{D \to NN\gamma} = ie\,\tilde{\mu}_{D \to NN}\,\epsilon_{ikl}F_{ik}\Psi_l^D\phi_1^\dagger\phi_2, \qquad (2)$$

where $\tilde{\mu}$ is the value of the transition magnetic moment assumed to be of the same order as μ_p, $F_{ik} = e_iq_k - e_kq_i$ is the electromagnetic field strength, and Ψ_l^D, ϕ_1, and ϕ_2 are the respective wave functions of the dibaryon and the nucleons. For the width of this direct decay, we then obtain

$$\Gamma_{D \to NN\gamma} = \alpha\Delta M^2\frac{\tilde{\mu}_{D \to NN}^2}{945\pi^2}(\Delta/M)^{7/2} \qquad (3)$$

which is numerically less than 0.1 eV for

$$\mu \sim \mu_p - \mu_n \approx 4.7/2M_N;$$

here, $\Delta = M_D - 2M$ is the energy release, or the maximum energy of the emitted photon. This estimate agrees with that made previously [14], but the final state interaction could increase it by several orders of magnitude.

To roughly take it into account, one must consider the transition $D \to d'$, where d' is the spin-zero quasideuteron, or $D^+ \to d$. At this point, an important statement is that the isovector magnetic transition operator for any skyrmion is simply related to its mixed, or interference inertia tensor Θ_{ab}^{int}. This statement, known in some particular cases [8, 10] is proved in Appendix B for arbitrary skyrmions and for any type of chiral soliton models: we show that

$$\tilde{\mu}_i^a = -\frac{1}{2}R^{aj}(A)\Theta_{jk}^{int}O_i^k(A'), \qquad (4)$$

where $R^{aj} = D_{aj}^1 = \text{Tr}(A^\dagger\tau^aA\tau^j)/2$, O_i^k are the final rotation matrices, and a is the isotopical (octet in $SU(3)$) index (for the electromagnetic interaction, we must set $a = 3$). Θ_{jk}^{int} is given in Appendix A.

For configurations with the generalized axial symmetry and for several known multiskyrmions, only the diagonal elements of Θ^{int} are different from zero, and moreover, only the 33-component remains in the axially symmetric case; we then have

$$\tilde{\mu}_i^3 = -\frac{1}{2}R^{33}(A)\Theta_{33}^{int}O_i^3(A'), \qquad (5)$$

where $\Theta_{33}^{int} = 2\Theta_{33}^I = 14.8$ GeV^{-1} for $B = 2$ and the accepted values of model parameters, see also Table 1 below. To obtain numerical values of the transition magnetic moments, we must calculate the rotation matrix elements between the wave functions of the initial

501

and final states. In terms of the final rotation matrices $D^I_{I_3,L}$, these are given by (see, e.g., [20])

$$\Psi^D_{I,I_3;J,J_3} = \sqrt{\frac{2I+1}{8\pi^2}} D^I_{I_3 L} \sqrt{\frac{2J+1}{8\pi^2}} D^J_{J_3,-2L}. \quad (6)$$

For the D state, we have $I = J = 1$ and $L = 0$, and for the final d' state, $I = 1$ and $J = 0$. Because $R^{33} = D^1_{00}$, the isotopical part of the matrix element for the $D \to d'$ transition is proportional to

$$\langle D^1_{I_3 0} D^1_{00} D^1_{I_3 0} \rangle = \int D^1_{I_3 0} D^1_{00} D^1_{I_3 0} d\nu =$$
$$= C^{1,I_3}_{1,0;1,I_3} C^{1,0}_{1,0;1,0}/3. \quad (7)$$

One of the Clebsch–Gordan coefficients vanishes, $C^{1,0}_{1,0;1,0} = 0$, and therefore, the $D \to d'$ transition magnetic moment is equal to zero for all states including D^{++} and D^0, not only for $D^+ \to d'^+$ (which is trivial); this is a consequence of symmetry properties of the rotator wave function with $L = 0$.

For the transition $D^+ \to d\gamma$, the isotopical part of the matrix element differs from zero, $\langle D^1_{0,0} D^1_{00} D^0_{00} \rangle = 1/3$, but the angular momentum part proportional to $\langle D^1_{J_3 0} D^1_{00} D^1_{J_3 0} \rangle$ is again equal to zero. However, the decay $D^+ \to np$ is possible as a result of the second-order isospin violation in the electromagnetic interaction, due to a virtual emission and reabsorption of the photon and due to the isospin violation by the mass difference of the u and d quarks. The order of magnitude estimate of the width of this decay due to the virtual electromagnetic process is

$$\Gamma_{D \to pn} \approx \alpha^2 \frac{M}{4\pi} \sqrt{\frac{\Delta}{M}}, \quad (8)$$

which is about ~ 1 keV. We note that for the components of D with the charge $+2$ or 0, the decay into the pp or nn final states is strictly forbidden by the rigorous conservation of the angular momentum and by the Pauli principle.

For the transitions

$$D^{++} \to pp\gamma, \quad D^0 \to nn\gamma,$$

and

$$D^+ \to (pn)_{I=1}\gamma,$$

the isoscalar magnetic moment operator gives a nonzero contribution. The corresponding matrix element is

$$M_{D \to d'\gamma} = ie\, \tilde{\mu}^0_{D \to d'}\, \epsilon_{ikl} F_{ik} \Psi^D_l \Psi^{d'\dagger}. \quad (9)$$

For the rational map parameterization, we have the approximate relation

$$\tilde{\mu}^0_3 \approx J_3 \frac{B \langle r_0^2 \rangle}{3\Theta^J}, \quad (10)$$

where $\langle r_0^2 \rangle$ is the mean square radius of the B-number distribution. Equation (10) coincides with the result in [8] for $B = 1$ and is close to the result in [10] for $B = 2$. The derivation of (10) that is valid for the rational map parameterization of skyrmions will be given elsewhere. The coefficient after J_3 in (10) has a remarkably weak dependence on the baryon number, as can be seen from Table 1. However, numerically, Eq. (10) gives about half the result for $B = 1$ in [8] for the parameters taken here. We thus have

$$\tilde{\mu}^0_{D \to d'} \approx \frac{2\langle r_0^2 \rangle}{3\Theta^J}. \quad (11)$$

For the decay width, we then obtain

$$\Gamma_{D \to d'\gamma} = \alpha \frac{4\tilde{\mu}^2_{D \to d'} \Delta^3}{3}. \quad (12)$$

Numerically, $\tilde{\mu}_{D \to d'} \approx 0.35$ GeV^{-1}, and it follows from (12) that $\Gamma_{D \to d'\gamma} \approx 0.3$ keV ($\Delta/60$ MeV)^3. The same estimate is valid for the decay rate of $D^+ \to np\gamma$ with the np-system in the $I = 1$ isospin state.

The experimental evidence for the existence of the narrow dibaryon D in the reaction $pp \to pp\gamma\gamma$ has been obtained in Dubna [21], although these data have not been confirmed in the Uppsala bremsstrahlung experiment [22]. Even more clear indications for the existence of low-lying dibaryons were obtained in the experiment at the Moscow meson factory in the reaction $pd \to pX$ [23]. As regards its importance, the confirmation of these results is comparable to the discovery of a new elementary particle. The absence of such states would provide definite restrictions on the applicability of the chiral soliton approach and effective field theories.

It should be noted that the model involves a problem with the lowest state with $I = J = 0$, which should be lower than the deuteron-like state. The deuteron must therefore decay into this $(0,0)$ state and a photon, but a two-nucleon system in the singlet $^1S_0$ state cannot decay because the $0 \to 0$ transition is forbidden for the electromagnetic interaction. The loop corrections to the energy of states, or the Casimir energy [16], are different for states that can go over into two nucleons, and for states that cannot. Their contribution can change the relative position of these states and shift the $(0,0)$ state above the deuteron, but a highly nontrivial calculation must be done to verify this.

Some low-lying states with strangeness are also predicted that cannot decay strongly due to the parity and isospin conservation in strong interactions [14]. For example, the dibaryon with the strangeness $S = -2$, $I = 0$, and $J = 1$ and with the positive parity has the energy by ≈ 0.17 GeV above the $\Lambda\Lambda$ threshold [24], and it cannot decay into two Λ-hyperons because of the Pauli principle, and into the $\Lambda\Lambda\pi$ final state by the isospin conservation. Therefore, the width of the electromagnetic decay of this state must not exceed several tenths of keV. It is, of course, a special case. Other possible states with the flavor s, c or b are discussed in the next section.

The masses of neutron-rich light nuclides, such as the tetra-neutron, sexta-neutron, etc., can be estimated using Eq. (1). For the multineutron state with $I = B/2$, the isorotation energy is

$$E^{rot} = \frac{B(B+2)}{8\Theta_I},$$

and these nuclides are predicted well above the threshold for the strong decay into final nucleons. With increasing the baryon numbers, the energies of neutron-rich states with a fixed difference $N - Z$ decrease, and their widths can therefore be very small. The mass difference of states with the isospin I and the ground states with $I = 0$ (for even B) is equal to

$$\Delta E(B, I) = \frac{I(I+1)}{2\Theta_{I,B}}.$$

For the pairs of nuclei such as ^{8}Li–^{8}Be, ^{12}B–^{12}C and ^{16}N–^{16}O, it is equal to

$$\Delta E(B, 1) = \frac{1}{\Theta_{I,B}}$$

and decreases with increasing B (i.e., the atomic number), both theoretically (see Table 1 below) and according to data. For $B = 16$, this difference is 10.9 MeV; this is to be compared with the theoretical value of 15.8 MeV, which is not bad for such a crude model.

3. FLAVORED MULTIBARYONS

Another characteristic prediction is that of multibaryons with different values of flavors, such as the strangeness, charm, or bottom quantum numbers. The bound-state approach of multiskyrmions with different flavors is an adequate method to calculate the binding energies of states with quantum numbers s, c or b. The so-called rigid oscillator model is the most transparent

and controllable version of this method [25]. The references to the pioneering papers can also be found in [26]. For the strangeness quantum numbers, the predicted binding energies of flavored states are smaller than the binding energies of the ordinary nuclei. For the charm or bottom quantum numbers, the relation is reversed. We now present the main results for flavored multibaryons following [26] and extending them to higher values of the baryon numbers.

To quantize solitons in the $SU(3)$ configuration space in the spirit of the bound-state approach to the description of strangeness, we consider the collective coordinate motion of the meson fields incorporated into a matrix $U \in SU(3)$ (see Appendix A),

$$
\begin{aligned}
U(r,t) &= R(t)U_0(O(t)\mathbf{r})R^{\dagger}(t), \\
R(t) &= A(t)S(t),
\end{aligned}
\tag{13}
$$

where U_0 is the $SU(2)$ soliton embedded into $SU(3)$ in the standard way (into the upper-left corner), $A(t) \in SU(2)$ describes $SU(2)$ rotations, $S(t) \in SU(3)$ describes rotations in the «strange», «charm» or «bottom» directions, and $O(t)$ describes rigid rotations in real space. We have

$$S(t) = exp(i\mathcal{D}(t)), \quad \mathcal{D}(t) = \sum_{a=4,\dots,7} D_a(t)\lambda_a, \tag{14}$$

where λ_a are the Gell-Mann matrices of the (u, d, s), (u, d, c) or (u, d, b) $SU(3)$ groups. The (u, d, c) and (u, d, b) $SU(3)$ groups are totally similar to the (u, d, s) one. For the (u, d, c) group, a simple redefiniton of the hypercharge must be made. For the (u, d, s) group,

$$D_4 = \frac{K^+ + K^-}{\sqrt{2}}, \quad D_5 = i\frac{K^+ - K^-}{\sqrt{2}},$$

etc., and for the (u, d, c) group,

$$D_4 = \frac{D^0 + \bar{D}^0}{\sqrt{2}},$$

etc.

The angular velocities of the isospin rotations are defined in the standard way as

$$A^{\dagger}\dot{A} = -i\boldsymbol{\omega} \cdot \boldsymbol{\tau}/2.$$

We do not consider the usual space rotations explicitly because the corresponding inertia moments for baryonic systems are much greater than the isospin inertia moments, see Table 1, and for the lowest possible values of the angular momentum J, the corresponding quantum correction is either exactly zero (for even B) or small.

The magnitude of the D field is small, at least of the order $1/\sqrt{N_c}$, where N_c is the number of QCD colors. We can therefore safely expand the matrix S in D. To the lowest order in D, the Lagrangian of the model in Eq. (A.1) can be written as

$$L = -M_{cl,B} + 4\Theta_{F,B}\dot{D}^\dagger \dot{D} -$$
$$- \left[\Gamma_B \bar{m}_D^2 + \tilde{\Gamma}_B(F_D^2 - F_\pi^2)\right]D^\dagger D -$$
$$- i\frac{N_c B}{2}(D^\dagger \dot{D} - \dot{D}^\dagger D), \quad (15)$$

where

$$\bar{m}_D^2 = (F_D^2/F_\pi^2)m_D^2 - m_\pi^2.$$

Here and below, D is the doublet K^+, K^0 (D^0, D^- or B^+, B^0) and Θ_F is the inertia moment for the rotation into the «flavor» direction (with $F = s$, c or b and the index c denoting the charm quantum number, except in N_c),

$$\Theta_{F,B} = \frac{1}{8}\int (1 - c_f) \times$$
$$\times \left[F_D^2 + \frac{1}{e^2}\left((\nabla f)^2 + s_f^2(\nabla n_i)^2\right)\right]d^3r, \quad (16)$$

where f is the profile function of the skyrmion, F_D is the flavor decay constant, i.e., kaon, D meson, or B meson decay constant, and

$$\Gamma_B = \frac{F_\pi^2}{2}\int (1 - c_f)d^3r. \quad (17)$$

The mass term contribution to the static soliton energy is related to Γ by

$$M.t. = m_\pi^2 \Gamma/2.$$

The quantity $\tilde{\Gamma}_B$ arises when the flavor symmetry breaking is taken into account in flavor decay constants:

$$\tilde{\Gamma}_B = \frac{1}{4}\int c_f\left[(\nabla f)^2 + s_f^2(\nabla n_i)^2\right]d^3r. \quad (18)$$

It is related to other calculated quantities by

$$\tilde{\Gamma} = 2(M_{cl}^{(2)}/F_\pi^2 - e^2\Theta_F^{Sk}),$$

where $M_{cl}^{(2)}$ is the second-order contribution to static mass of the soliton and Θ_F^{Sk} is the Skyrme term contribution to the flavor inertia moment. The contribution proportional to $\tilde{\Gamma}_B$ is suppressed in (15) compared to the term $\sim \Gamma$ by the small factor $\sim F_D^2/m_D^2$, and is more important for strangeness. The term proportional to $N_c B$ arises in (15) from the Wess–Zumino term in the action and is responsible for the difference of the

strangeness and antistrangeness (in the general case, flavor and antiflavor) excitation energies [25, 26].

Following the canonical quantization procedure, we write the Hamiltonian of the system including the terms of the order N_c^0 as [25]

$$H_B = M_{cl,B} + \frac{1}{4\Theta_{F,B}}\Pi^\dagger \Pi +$$
$$+ \left(\Gamma_B \bar{m}_D^2 + \tilde{\Gamma}_B(F_D^2 - F_\pi^2) + \frac{N_c^2 B^2}{16\Theta_{F,B}}\right)D^\dagger D +$$
$$+ i\frac{N_c B}{8\Theta_{F,B}}(D^\dagger \Pi - \Pi^\dagger D), \quad (19)$$

where Π is the canonically conjugate momentum to the variable D that describes the oscillator-type motion of the (u,d) $SU(2)$ soliton in the $SU(3)$ configuration space. After the diagonalization that can be done explicitly [25], the normal-ordered Hamiltonian can be written as

$$H_B = M_{cl,B} + \omega_{F,B}a^\dagger a + \bar{\omega}_{F,B}b^\dagger b + O(1/N_c), \quad (20)$$

where $a^\dagger$ and $b^\dagger$ are the creation operators of the strangeness (i.e., of antikaons) and antistrangeness (flavor and antiflavor) quantum numbers, and $\omega_{F,B}$ and $\bar{\omega}_{F,B}$ are the frequences of flavor (antiflavor) excitations. D and Π are related to a and b by [25]

$$D^i = \frac{b^i + a^{\dagger i}}{\sqrt{N_c B \kappa_{F,B}}}, \quad \Pi^i = \frac{\sqrt{N_c B \kappa_{F,B}}(b^i - a^{\dagger i})}{2i} \quad (21)$$

with

$$\kappa_{F,B} = \sqrt{1 + \frac{16(\bar{m}_D^2 \Gamma_B + (F_D^2 - F_\pi^2)\tilde{\Gamma}_B \Theta_{F,B})}{(N_c B)^2}}.$$

For the lowest states, the values of D are small:

$$D \sim \left[16\Gamma_B \Theta_{F,B}\bar{m}_D^2 + N_c^2 B^2\right]^{-1/4};$$

they increase as $(2|F| + 1)^{1/2}$ with increasing the flavor number $|F|$. As noted in [25], deviations of the field D from the vacuum decrease with increasing the mass m_D, as well as with increasing the number of colors N_c, and the method works for any m_D (and also for charm and bottom quantum numbers). We have

$$\omega_{F,B} = \frac{N_c B(\kappa_{F,B} - 1)}{8\Theta_{F,B}},$$
$$\bar{\omega}_{F,B} = \frac{N_c B(\kappa_{F,B} + 1)}{8\Theta_{F,B}}. \quad (22)$$

It was observed in [26] that to the leading order in N_c, the difference

$$\bar{\omega}_{F,B} - \omega_{F,B} = \frac{N_c B}{4\Theta_{F,B}}$$

Table 1.   Characteristics of the bound states of skyrmions with the baryon numbers up to $B = 22$

B	M_{cl}	$\Theta_F^{(0)}$	Θ_I	$\Theta_{I,3}$	$\bar{\Theta}_J$	Γ	$\tilde{\Gamma}$	$\langle r_0 \rangle$	ω_s	ω_c	ω_b
1	1.702	2.05	5.55	5.55	5.55	4.80	15	2.51	0.309	1.542	4.82
2	3.26	4.18	11.5	7.38	23	9.35	22	3.46	0.293	1.511	4.76
3	4.80	6.34	14.4	14.4	49	14.0	27	4.10	0.289	1.504	4.75
4	6.20	8.27	16.8	20.3	78	18.0	31	4.53	0.283	1.493	4.74
5	7.78	10.8	23.5	19.5	126	23.8	35	5.10	0.287	1.505	4.75
6	9.24	13.1	25.4	27.7	178	29.0	38	5.48	0.287	1.504	4.75
7	10.6	14.7	28.9	28.9	220	32.3	43	5.72	0.282	1.497	4.75
8	12.2	17.4	33.4	31.4	298	38.9	46	6.15	0.288	1.510	4.79
9	13.9	20.5	37.7	37.7	375	46	47	6.49	0.291	1.517	4.77
12	18.4	28.0	48.5	48.5	636	64	54	7.31	0.294	1.526	4.79
16	24.5	38.9	63.1	63.1	1107	91	63	8.31	0.301	1.543	4.81
17	25.9	41.2	66.1	66.1	1219	96	65	8.48	0.300	1.542	4.81
22	33.7	56.0	84.2	84.2	2027	135	73	9.55	0.308	1.560	4.84
32*	49.1	86.7	118	118	4154	218	87	11.3	0.319	1.585	4.84

The classical mass of solitons M_{cl} is expressed in GeV, the moments of inertia Θ_F, Θ_I and $\Theta_{I,3}$, Θ_J, $\langle r_0 \rangle$, Γ, and $\tilde{\Gamma}$ in GeV^{-1}, and the excitation frequencies for flavor F, $\omega_{s,c,b}$ in GeV; $\langle r_0 \rangle = \sqrt{r_B^2}$, Θ_J defines the value of the multiskyrmion isoscalar magnetic moment. For higher baryon numbers, beginning with $B = 9$, calculations are made using the RM ansatz. For $B = 32$, it was assumed that the ratio $\mathcal{I}/B^2 = 1.28$ as for the RM $B = 22$ skyrmion. The external parameters of the model are $F_\pi = 186$ MeV and $e = 4.12$. The accuracy of calculations is better than 1% for the masses and several per cent for other quantities.

coincides with the expression obtained in the collective coordinate approach [24].

The flavor symmetry breaking (FSB) in the flavor decay constants, i.e., the fact that $F_K/F_\pi \approx 1.22$ and $F_D/F_\pi = 1.7 \pm 0.2$ (where we take $F_D/F_\pi = 1.5$ and $F_B/F_\pi = 2$) leads to the increase of the flavor excitation frequences, in better agreement with the data for charm and bottom. It also leads to some increase of the binding energies of baryon system [26].

The values of $\bar{\Theta}_J$ shown in Table 1 are $1/3$ of the trace of the corresponding inertia tensor, see Appendix A. As can be seen from Table 1, the flavor excitation energies increase again for the largest value $B = 22$, and the important property of binding becomes weaker for higher B. However, this can be an artefact of the RM approximation discussed in the next section. In particular, for $B \geq 9$, the inertia moments Θ_I and Θ_3 are $1/3$ of the trace of the corresponding inertia tensors, see Appendix A.

For large values of $F_D/F_\pi = \rho_D$ and the mass m_D, the following approximate formula for the flavor excitation frequences can be obtained:

$$\omega_{F,B} \approx \tilde{m}_D \left(1 - 2\frac{\Theta_{F,B}^{Sk}}{\rho_D^2 \Gamma_B} \right) - \frac{N_c B}{2\rho_D^2 \Gamma_B} \qquad (23)$$

with $\tilde{m}_D^2 = m_D^2 + F_\pi^2 \tilde{\Gamma}_B/\Gamma_B$. It is clear from (23) that ω's are smaller than the meson masses m_D, and therefore, the binding always occurs and is to a large degree due to the contribution of the Skyrme term to the flavor inertia Θ_F^{Sk}. As $\rho_D \to \infty$, it follows that $\omega_F \to m_D$. Because the ratio $\tilde{\Gamma}_B/\Gamma_B$ decreases with increasing B and $\Theta_{F,B}/\Gamma_B$ increases as B increases from 1 to 4–7, the energies $\omega_{F,B}$ decrease for these B numbers, thereby leading to the increase of the binding of flavored mesons by $SU(2)$ solitons with increasing B up to 4–7. However, for $B = 22$ and 32, the ratio $\Theta_{F,B}/\Gamma_B$ is smaller than for $B = 1$, and indeed, ω's are the same and even larger than for $B = 1$.

Table 2.   The binding energy differences $\Delta\epsilon_{s,c,b}$ for the states with the isospin $I = T_r + |F|/2$

B	$\Delta\epsilon_{s=-1}$	$\Delta\epsilon_{c=1}$	$\Delta\epsilon_{b=-1}$	$\Delta\epsilon_{s=-2}$	$\Delta\epsilon_{c=2}$	$\Delta\epsilon_{b=-2}$
2	-0.047	-0.03	0.02	-0.053	-0.07	0.02
3	-0.042	-0.01	0.04	-0.036	-0.03	0.06
4	-0.020	0.019	0.06	-0.051	0.022	0.10
5	-0.027	0.006	0.05	-0.063	0.001	0.08
6	-0.019	0.016	0.05	-0.045	0.023	0.10
7	-0.016	0.021	0.06	-0.041	0.033	0.11
8	-0.017	0.014	0.02	-0.040	0.021	0.03
9	-0.023	0.005	0.03	-0.10	-0.003	0.06
12	-0.021	0.003	0.02	-0.09	-0.004	0.04
17	-0.027	-0.013	0.00	-0.11	-0.03	-0.00
22	-0.034	-0.028	-0.03	-0.14	-0.06	-0.03

The binding energy differences $\Delta\epsilon_{s,c,b}$ are the changes of binding energies of the lowest baryon system with the flavor s, c or b and the isospin $I = T_r + |F|/2$ compared to the usual u, d nuclei, for the flavor numbers $S = -1, -2$, $c = 1, 2$, $b = -1$ and -2 (see Eq. (24)). The $SU(3)$ multiplets are $(p, q) = (0, 3B/2)$ for even B and $(p, q) = (1, (3B - 1)/2)$ for odd B.

Table 3.   The binding energy differences for the states with the isospin $I = 0$

B	$\Delta\epsilon_{s=-1}$	$\Delta\epsilon_{c=1}$	$\Delta\epsilon_{b=-1}$	$\Delta\epsilon_{s=-2}$	$\Delta\epsilon_{c=2}$	$\Delta\epsilon_{b=-2}$	$\Delta\epsilon_{s=-3}$	$\Delta\epsilon_{c=3}$	$\Delta\epsilon_{b=-3}$	$\Delta\epsilon_{s=-B}$
2	—	—	—	-0.075	-0.03	0.02	—	—	—	-0.07
3	0.000	0.034	0.07	—	—	—	-0.08	0.002	0.09	-0.08
4	—	—	—	-0.047	0.030	0.09	—	—	—	-0.13
5	-0.003	0.032	0.06	—	—	—	-0.06	0.035	0.12	-0.15
6	—	—	—	-0.044	0.025	0.09	—	—	—	-0.21
7	0.000	0.040	0.07	—	—	—	-0.04	0.068	0.15	-0.20
8	—	—	—	-0.039	0.023	0.03	—	—	—	-0.28
12	—	—	—	-0.046	0.00	0.03	—	—	—	-0.50
17	-0.020	-0.01	-0.00	—	—	—	-0.08	-0.04	-0.01	-0.82
22	—	—	—	-0.073	-0.06	-0.06	—	—	—	-1.3
32*	—	—	—	-0.088	-0.11	-0.13	—	—	—	$--$

The binding energy differences between the lowest flavored baryon system with the isospin $I = 0$ and the ground state with the same value of B and $I = 0$ or $I = 1/2$. The first three columns are for $|F| = 1$, the next three columns for $|F| = 2$, and the next three for $|F| = 3$. The state with the flavor value $|F|$ belongs to the $SU(3)$ multiplet with $T_r = |F|/2$. In the last column, the binding energy differences are shown for the isoscalar electrically neutral states with $S = -B$. For $|F| \geq 3$, all estimates are very approximate.

The binding energy differences between flavored multibaryons and the ordinary nuclei in the rigid oscillator approximation are given by

$$\Delta\epsilon_{B,F} = |F|\left[\omega_{F,1} - \omega_{F,B} - \frac{3(\kappa_{F,1} - 1)}{8\kappa_{F,1}^2\Theta_{F,1}} - \right.$$
$$\left. - \frac{T_r(\kappa_{F,B} - 1)}{4\kappa_{F,B}\Theta_{F,B}} - \frac{(|F| + 2)(\kappa_{F,B} - 1)^2}{8\kappa_{F,B}^2\Theta_{F,B}}\right], \quad (24)$$

and the lowest $SU(3)$ multiplets are considered with the isospin of the flavorless component $T_r = 0$ for even B and $T_r = 1/2$ for odd B. This formula is correct for $|F| = 1$ and for any $|F|$ if the baryon number is sufficiently large to ensure the isospin balance.

The values of $\Delta\epsilon$ shown in Table 2 must be considered as an estimate. They illustrate the restricted possibilities of the RM approximation for large-B multiskyrmions.

The isosinglet baryon systems, in particular those with $|F| = B$, are of special interest. As argued in [26], these states do not belong to the lowest possible $SU(3)$ irreducible representations, they must have $T_r = |F|/2$. It makes sense to calculate the difference between the binding energy of this state and the minimal state (p^{min}, q^{min}) with zero flavor, which we identify with the standard nucleus (the ground state). We have

$$\Delta\epsilon_{B,F} = |F|\left[\omega_{F,1} - \omega_{F,B} - \frac{3(\kappa_{F,1} - 1)}{8\kappa_{F,1}^2\Theta_{F,1}} + \right.$$
$$\left. + \frac{(|F| + 2)(\kappa_{F,B} - 1)}{8\kappa_{F,B}^2\Theta_{F,B}}\right] -$$
$$- \frac{1}{2\Theta_{T,B}}\left[\frac{|F|(|F| + 2)}{4} - T_r^{min}(T_r^{min} + 1)\right], \quad (25)$$

where $T_r^{min} = 0$, or $1/2$ as above.

According to Table 3, the total binding energy, e.g., of the state with $B = 22$ and $S = -2$ is smaller than that of the nucleus with $A = 22$ by 73 MeV, and this state must therefore be well bound. The model used here is too crude for large flavor values, and the results obtained can be used only as an illustration and as a starting point for further investigations. Similar results are also obtained in other versions of the model [27], in particular in the quark–meson soliton model [28]. For the baryon numbers $B = 3, 4$, estimates of the spectra of baryonic systems with the charm quantum number were made in [29] within the conventional quark model. They are in a relatively good agreement with ours.

In the channel with $B = 2$, the near-threshold state with the strangeness $S = -1$ was observed a long time ago in the reaction $pp \rightarrow p\Lambda K^+$ [30] and recently

confirmed in COSY experiment [31]. A similar near-threshold $\Lambda\Lambda$ state was observed by the KEK PS E224 collaboration [32]. The Skyrme model explains these near-threshold states with $B = 2$ and predicts similar states for higher values of B. For some values of B beginning with $B \geq 5, 6$, such states with several units of strangeness can be stable with respect to strong interactions. Because of the well-known relation $Q = I_3 + (B+S)/2$ between the charge, the isospin, and the hypercharge of hadrons, the baryon system with several units of strangeness can appear as negatively charged nuclear fragments. For even B and the minimal multiplets $(p, q) = (0, 3B/2)$, the strangeness is $S = -2I$, and the condition for the $Q = -1$ fragment to appear is $-1 = S + B/2$, or $-S = B/2 + 1$. For $B = 6$, this gives $S = -4$, for $B = 8$, $S = -5$, etc. For odd B, the $Q = -1$ state must have the strangeness

$$|S| = (B - 1)/2 + 1,$$

i.e., -3, -4, and -5 for $B = 5$, 7, and 9, etc.

The negatively charged long-lived nuclear fragment with the mass about 7.4 GeV observed in NA52 CERN experiment in a Pb + Pb collision at the energy $158A$ GeV [33] can be, within the chiral soliton models, a fragment with $B = 7$ or 6 and the strangeness $S = -4$ or $-5, -6$. The confirmation of this result and the search for other negatively charged fragments would be of great importance. For the charm or bottom quantum numbers, the binding energies are greater, but observing these states requires considerably higher incident energies.

4. LARGE-B MULTISKYRMIONS FROM RATIONAL MAPS IN THE DOMAIN-WALL APPROXIMATION

The treatment of multiskyrmions was considerably simplified by extensively using the rational map ansatz proposed in [15] (and also adopted in the present paper). At the same time, this ansatz leads to the picture of the multibaryon system at large B that is probably incompatible with the picture for the ordinary nuclei. To clarify this point, we here consider large-B multiskyrmions in some kind of a toy model — in the domain-wall approximation; in spite of its simplicity, this model gives relatively good numerical results for the known RM multiskyrmions except those with $B = 1, 2$. Within the rational map ansatz [15], the energy of the skyrmion is given by

$$M = \frac{1}{3\pi}\int\left\{A_N r^2 f'^2 + 2B s_f^2(f'^2 + 1) + \mathcal{I}\frac{s_f^4}{r^2}\right\}dr \quad (26)$$

in the universal units $3\pi^2 F_\pi/e$.

The coefficient $A_N = 2(N-1)/N$ corresponds to the symmetry group $SU(N)$ [34]. For $SU(2)$, the quantity $\mathcal{I}$ is given in Appendix A. There is the inequality $\mathcal{I} \geq B^2$. Direct numerical calculations have shown and our analytical treatment supports that at large B, and hence, large $\mathcal{I}$, the multiskyrmion looks like a spherical ball with the profile given by $f = \pi$ inside and $f = 0$ outside the ball. The energy and the B-number density of this configuration is concentrated at its boundary, similarly to the domain wall system considered in [35] in connection with cosmological problems.

We consider such a large-B skyrmion within the «inclined step» approximation. If W is the width of the step and r_0 is the radius of the skyrmion (where the profile is given by $f = \pi/2$), we have

$$f = \pi/2 - (r - r_0)\pi/W \quad \text{for} \quad r_0 - W/2 \leq r \leq r_0 + W/2.$$

We note that this approximation describes the usual domain wall energy [35] with the accuracy $\sim 9\%$.

We write the energy in terms of W and r_0 and then minimize it with respect to both these parameters and find the minimum energy value. With

$$M(W, r_0) =$$
$$= \frac{1}{3\pi}\left[\frac{\pi^2}{W}(B + A_N r_0^2) + W\left(B + \frac{3\mathcal{I}}{8r_0^2}\right)\right], \quad (27)$$

this gives

$$W_{min} = \pi\left[\frac{B + A_N r_0^2}{B + 3\mathcal{I}/8r_0^2}\right]^{1/2} \quad (28)$$

and after the minimization,

$$r_{0\,min}^2 = \sqrt{\frac{3\mathcal{I}}{8A_N}}.$$

In dimensional units, we then have

$$r_0 = \frac{(6\mathcal{I}/A_N)^{1/4}}{F_\pi e}.$$

Because $\mathcal{I} \geq B^2$, the radius of the minimized configuration grows at least as $\sqrt{B}$. It follows that $W_{min} = \pi$, which is therefore independent of B for any $SU(N)$. The energy is given by

$$M_{min} \approx \frac{2B + \sqrt{3A_N\mathcal{I}/2}}{3}. \quad (29)$$

For the $SU(2)$ model, $A_N = 1$ and the energy $M_{min} = (2B + \sqrt{3\mathcal{I}/2})/3$ should be compared with the lower bound $M_{LB} = (2B + \sqrt{\mathcal{I}})/3$. The formula gives

the numbers for $B = 3, \ldots, 22$ in a remarkably good agreement (within 2–3%) with the calculation within the RM approximation [7].

It is not difficult to calculate the corrections to these expressions, of the relative order $1/B$, $1/B^2, \ldots$:

$$M(W, r_0) \approx \frac{1}{3\pi}\left\{\frac{\pi^2}{W}(B + A_N r_0^2) + \right.$$
$$\left. + W\left[B(1 + \beta) + \frac{3\mathcal{I}}{8r_0^2}(1 + \gamma)\right]\right\}, \quad (30)$$

where

$$\beta = \frac{\pi^2}{12B}, \quad \gamma = \frac{2\pi^2 + 17}{\sqrt{24\mathcal{I}}}.$$

It follows that

$$M_{min} \approx [2B(1 + \beta/2) + \sqrt{3\mathcal{I}/2}(1 + \gamma/2)]/3. \quad (31)$$

However, the first-order correction in W does not improve the description of masses, and the summation of all terms seems to be required[1].

We thus see that a very simple approximation confirms the picture emerging from the numerical calculation of the RM skyrmion as a two-phase object, a spherical ball with the profile $f = \pi$ inside and $f = 0$ outside the ball, and a fixed-width envelope with the fixed surface energy density,

$$\rho_M \approx \frac{2B + \sqrt{3\mathcal{I}/2}}{12\pi r_0^2}.$$

We also consider the effect of the mass term. It gives the contribution

$$M.t. = \tilde{m}\int r^2(1 - \cos f)dr, \quad (32)$$

where

$$\tilde{m} = \frac{8m_\pi^2}{3\pi F_\pi^2 e^2}.$$

For the strangeness, charm or bottom, the masses m_K, m_D or m_B must be inserted instead of m_π. In the «inclined step» approximation, we then obtain

$$M.t. \approx \tilde{m}\left[\frac{2}{3}r_0^3 + O(W^2)\right]. \quad (33)$$

In view of this structure of the mass term, it does not affect the width of the step W in the lowest order, but the dimension of the soliton r_0 becomes smaller:

$$r_0 \to r_0 - \tilde{m}\frac{r_0^2(B + A_N r_0^2)}{4\pi B}. \quad (34)$$

[1] Detailed analytical treament of multiskyrmions performed by the author in Pis'ma v ZhETF **73**, 667 (2001) confirms the results and conclusions of this section.
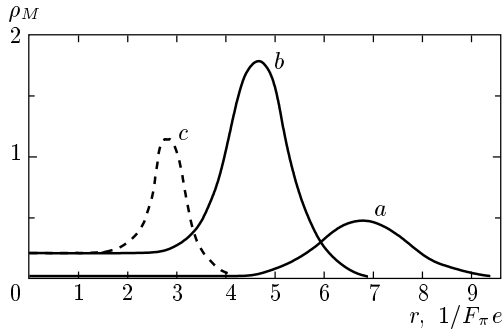
The mass density distribution of the rational map multiskyrmion with $B = 22$ as a function of the distance from the center of the skyrmion for different values of mass in the chiral symmetry breaking term; a — pion mass in the mass term, b — kaon mass, c — D-meson mass, the mass density is devided by 10

As was expected from general grounds, dimensions of the soliton decrease with increasing $\tilde{m}$. However, even for large values of $\tilde{m}$, the structure of the multiskyrmion remains the same at large B: it is given by the phase with the broken chiral symmetry inside the spherical wall where the main contribution to the mass and topological charge is concentrated. The behavior of the energy density for $B = 22$ at different values of μ is shown in the Figure. The value of the mass density inside the ball is completely determined by the mass term with $1 - c_f = 2$. The baryon number density distribution is quite similar, with the only difference that it is equal to zero inside the bag. It follows from these results that the RM-approximated multiskyrmions cannot model real nuclei at large B, probably for $B > 12 - 20$, and configurations of the skyrmion crystal type may be more appropriate for this purpose.

In addition to the simple one-shell configurations considered in [7, 15] and here, multishell configurations can also be interesting. Some examples of two-shell configurations with $B = 12, 13, 14$ were considered recently [36]. For these configurations, the profile is given by $f = 2\pi$ at $r = 0$ and decreases to $f = 0$ as $r \to \infty$. We can also model this two-shell configuration in the domain-wall, or spherical bag approximation with the result

$$M \approx \frac{2B_1 + \sqrt{3\mathcal{I}_1/2}}{3} + \frac{2B_2 + \sqrt{3\mathcal{I}_2/2}}{3}, \qquad (35)$$

with the total baryon number $B = B_1 + B_2$. The profile f decreases from 2π to π in the first shell, and from π to 0 in the second. The radii of both shells must satisfy the condition

$$r_0^{(2)} \geq r_0^{(1)} + W,$$

and the external shell must therefore be sufficiently large, with the baryon number B_2 given by several tens at least. Because the ratio $\mathcal{I}/B^2$ is larger for smaller B, the energy in Eq. (35) is greater than the energy of the one-shell configuration considered before. Calculations performed in [36] also did not improve the results obtained for the one-shell configuration. However, a more refined analysis would be of interest. The observation concerning the structure of large-B multiskyrmions made above can be useful in view of possible cosmological applications of Skyrme-type models.

5. CONCLUDING REMARKS

We have restricted ourselves to the Skyrme model and its straightforward extentions. However, many of the result are valid in other versions of the model, e.g., in the model with solitons stabilized by the explicit vector (ω) meson or by the baryon number density squared, in the chiral perturbation theory, etc., see the discussion in the second paper in Ref. [14]. The $B = 2$ torus-like configuration has been obtained within these models and in the chiral quark–meson model [28], and it would be interesting to check if there also exist multiskyrmions with $B \geq 3$.

We did not discuss a special class of $SU(3)$ skyrmions, the $SO(3)$ solitons and the problem of their observation. The relevant discussion can be found in [12, 13].

To conclude, the study of some processes, including those at intermediate energies, which to some extent are out of fashion now, can provide a very important check of fundamental principles and concepts of the elementary particle theory including the confinement of quarks and gluons. Confirming the predictions of the chiral soliton approach would give a qualitatively new understanding of the origin of nuclear forces. If the existence of low-energy radiatively decaying dibaryons is reliably established, it will change the long-standing belief that nuclear matter fragments necessarily consist of separate nucleons bound by their interactions. It is therefore extremely important to confirm and check the results of experiments on the dibaryon production and on the production of fragments of flavored matter. This would be possible at accelerators of moderate energies, like COSY (Juelich, FRG), KEK (Japan), Moscow meson factory (Troitsk, Russia), ITEP (Moscow), and several others. The production of multistrange states and the states with charm or bottom quantum numbers is

possible in heavy ion collisions and also on the accelerators like Japan Hadron Facility to be built in the near future.

The multiple flavor production realized in the production of flavored multibaryons that is possible, e.g., in heavy ion collisions, certainly requires higher energy, but multiple interaction processes and the normal Fermi motion of nucleons inside the nuclei make the effective thresholds much lower [37]. It would allow more complete and reliable verification of the model predictions.

We finally note that the low-energy dibaryons were recently obtained in [38] using a quantization procedure different from ours.

APPENDIX A

Inertia tensors of multiskyrmions

The Lagrangian density of the $SU(2)$ Skyrme model is given by

$$
\mathcal{L} = -\frac{F_\pi^2}{16} \operatorname{Tr}(L_\mu L_\mu) + \frac{1}{32e^2} \operatorname{Tr} G_{\mu\nu}^2 +
$$
$$
+ \frac{F_\pi^2 m_\pi^2}{16} \operatorname{Tr}(U + U^\dagger - 2), \quad (A.1)
$$

where $L_\mu = \partial_\mu U U^\dagger$ is the left chiral derivative, $L_\mu = iL_{\mu,k}\tau_k$, τ_k are the Pauli matrices, and $G_{\mu\nu} = \partial_\mu L_\nu - \partial_\nu L_\mu$ is the chiral field strengh. The Wess–Zumino term present in the action was discussed in detail in [13], and we omit this discussion here.

We first give the expression for the energy of the $SU(2)$ skyrmion as a function of the profile f and the unit vector **n**, which is especially useful in some cases. Using the definition $U = c_f + i s_f \mathbf{n} \cdot \boldsymbol{\tau}$ and the relation

$$
L_{\mu,k} L_{\nu,k} = \partial_\mu f \partial_\nu f + s_f^2 \partial_\mu \mathbf{n} \partial_\nu \mathbf{n}, \quad (A.2)
$$

we obtain

$$
M_{stat} = \int \left\{ \frac{F_\pi^2}{8} [(\nabla f)^2 + s_f^2 (\nabla n_i)^2] + \frac{s_f^2}{4e^2} \times \right.
$$
$$
\left. \times \left[2[\nabla f \times \nabla n_i]^2 + s_f^2 [\nabla n_i \times \nabla n_k]^2 \right] + \rho_{M.t.} \right\} d^3 r. \quad (A.3)
$$

For the ansatz based on rational maps, the profile f depends on only the variable r, and components of **n** depend only on the angular variables θ, ϕ. We have

$$
n_x = \frac{2 \operatorname{Re} R}{1 + |R|^2}, \quad n_y = \frac{2 \operatorname{Im} R}{1 + |R|^2}, \quad n_z = \frac{1 - |R|^2}{1 + |R|^2},
$$

where R is a rational function of the variable $z = \operatorname{tg}(\theta/2) \exp(i\phi)$ defining a map $S^2 \to S^2$. In this case, the gradients of f and **n** are orthogonal (recall that $\nabla_r = \mathbf{n}_r \partial_r + \mathbf{n}_\theta \partial_\theta / r + \mathbf{n}_\phi \partial_\phi / (r s_\theta)$, $\mathbf{n}_r = \mathbf{r}/r = (s_\theta c_\phi, s_\theta s_\phi, c_\theta)$, $\mathbf{n}_\theta = (-c_\theta c_\phi, -c_\theta s_\phi, s_\theta)$, and $\mathbf{n}_\phi = (s_\phi, -c_\phi, 0)$) and $[\nabla f \times \nabla n_1]^2 = f'^2 (\nabla n_1)^2$, etc. Using the relations

$$
n_3^2 [\nabla n_2 \times \nabla n_3]^2 = n_1^2 [\nabla n_1 \times \nabla n_2]^2,
$$
$$
n_3^2 [\nabla n_1 \times \nabla n_3]^2 = n_2^2 [\nabla n_1 \times \nabla n_2]^2, \quad (A.4)
$$

we can rewrite (A.3) as

$$
M_{stat} = \int \left\{ \frac{F_\pi^2}{8} [f'^2 + s_f^2 (\nabla n_i)^2] + \frac{s_f^2}{2e^2} \times \right.
$$
$$
\left. \times \left[f'^2 (\nabla n_i)^2 + \frac{s_f^2 [\nabla n_1 \times \nabla n_2]^2}{n_3^2} \right] + \rho_{M.t.} \right\} d^3 r. \quad (A.5)
$$

Introducing the notation

$$
\mathcal{I} = \frac{1}{4\pi} \int r^4 \frac{[\nabla n_1 \times \nabla n_2]^2}{n_3^2} d\Omega =
$$
$$
= \frac{1}{4\pi} \int \left(\frac{(1 + |z|^2)}{(1 + |R|^2)} \frac{|dR|}{|dz|} \right)^4 \frac{2i \, dz \, d\bar{z}}{(1 + |z|^2)^2} \quad (A.6)
$$

and using the equation

$$
\int r^2 (\nabla n_k)^2 d\Omega = 2 \int r^2 \frac{|[\nabla n_1 \times \nabla n_2]|}{|n_3|} d\Omega =
$$
$$
= 2 \int \frac{2i \, dR \, d\bar{R}}{(1 + |R|^2)^2} = 8\pi \mathcal{N}, \quad (A.7)
$$

we finally obtain

$$
M_{stat} = 4\pi \int \left\{ \frac{F_\pi^2}{8} (f'^2 r^2 + 2 s_f^2 \mathcal{N}) + \frac{s_f^2}{2e^2} \times \right.
$$
$$
\left. \times \left[2 f'^2 \mathcal{N} + \frac{s_f^2 \mathcal{I}}{r^2} \right] + r^2 \rho_{M.t.} \right\} dr. \quad (A.8)
$$

To find the minimum energy configuration at fixed $\mathcal{N} = B$, one minimizes $\mathcal{I}$ and then finds the profile $f(r)$ by minimizing energy (A.8).

To quantize zero modes, we use the ansatz

$$
U(t, r) = A(t) U(O_{ik}(t) r_k) A^\dagger(t)
$$

and the evident relation

$$\partial_t U = \dot{U} = \dot{A} U(\mathbf{r}(t)) A^\dagger + A U(\mathbf{r}(t)) \dot{A}^\dagger + \\ + \dot{r}_i(t) A \partial_i U(\mathbf{r}(t)) A^\dagger, \quad \text{(A.9)}$$

where $r_i(t) = O_{ik}(t) r_k$ are body-fixed coordinates.

The angular velocities of spatial (or orbital) rotations are introduced as

$$\dot{r}_i = \dot{O}_{ik} r'_k = \dot{O}_{ik} O_{kl}^{-1} r_l(t) = -\epsilon_{ilm} \Omega_m r_l(t)$$

and the integration is performed in the coordinate system bound to the soliton (body-fixed).

The rotation, or the zero-mode energy of $SU(2)$ skyrmions as a function of the angular velocities is

$$E_{rot} = \frac{1}{2} \Theta_{ab}^I \omega_a \omega_b + \Theta_{ab}^{int} \omega_a \Omega_b + \frac{1}{2} \Theta_{ab}^J \Omega_a \Omega_b. \quad \text{(A.10)}$$

The isotopical inertia tensor for an arbitrary $SU(2)$ skyrmion is given by

$$\Theta_{ab}^I = \int s_f^2 \left\{ (\delta_{ab} - n_a n_b) \times \right. \\ \left. \times \left(\frac{F_\pi^2}{4} + \frac{(\nabla f)^2}{e^2} \right) + \frac{s_f^2}{e^2} \partial_l n_a \partial_l n_b \right\} d^3 r. \quad \text{(A.11)}$$

For the RM ansatz, the trace of this inertia tensor is

$$\Theta_{aa}^I(RM) = 4\pi \int s_f^2 \times \\ \times \left\{ \frac{F_\pi^2}{2} + \frac{2}{e^2} \left(f'^2 + \mathcal{N} \frac{s_f^2}{r^2} \right) \right\} r^2 dr. \quad \text{(A.12)}$$

The orbital inertia tensor gives the contribution to the energy $\Theta_{ab}^J \Omega_a \Omega_b / 2$; using the same notation for an arbitrary configuration, we have

$$\Theta_{ab}^J = \int \left\{ \frac{F_\pi^2}{4} (\partial_i f \partial_k f + \right. \\ + s_f^2 \partial_i \mathbf{n} \partial_k \mathbf{n}) + \frac{s_f^2}{e^2} \left[\partial_i f \partial_k f (\nabla n_l)^2 + (\nabla f)^2 \partial_i \mathbf{n} \partial_k \mathbf{n} - \right. \\ - \partial_i f \partial_l f \partial_l \mathbf{n} \partial_k \mathbf{n} - \partial_k f \partial_l f \partial_l \mathbf{n} \partial_i \mathbf{n} + \\ \left. + s_f^2 [(\nabla n_l)^2 \partial_i \mathbf{n} \partial_k \mathbf{n} - (\partial_i \mathbf{n} \partial_l \mathbf{n})(\partial_k \mathbf{n} \partial_l \mathbf{n})] \right] \right\} \times \\ \times \epsilon_{i\alpha a} \epsilon_{k\beta b} r_\alpha r_\beta d^3 r. \quad \text{(A.13)}$$

For the RM ansatz, this expression can be simplified as

$$\Theta_{ab}^J = \int s_f^2 \left\{ \left[\frac{F_\pi^2}{4} + \frac{f'^2}{e^2} + \frac{s_f^2}{e^2} (\nabla n_l)^2 \right] \times \\ \times \left[(\nabla n_l)^2 (r^2 \delta_{ab} - r_a r_b) - \partial_a \mathbf{n} \partial_b \mathbf{n} r^2 \right] - \\ - \frac{s_f^2}{e^2} \left[(\partial_i \mathbf{n} \partial_k \mathbf{n})(\partial_i \mathbf{n} \partial_k \mathbf{n})(r^2 \delta_{ab} - r_a r_b) - \\ - r^2 (\partial_a \mathbf{n} \partial_l \mathbf{n})(\partial_b \mathbf{n} \partial_l \mathbf{n}) \right] \right\} d^3 r. \quad \text{(A.14)}$$

This allows us to obtain the trace of the inertia tensor

$$\Theta_{aa}^J(RM) = 4\pi \int s_f^2 \times \\ \times \left\{ \frac{F_\pi^2}{2} \mathcal{N} + \frac{2}{e^2} \left(f'^2 \mathcal{N} + \mathcal{I} \frac{s_f^2}{r^2} \right) \right\} r^2 dr. \quad \text{(A.15)}$$

It is easy to establish inequality for the the traces of isotopical and orbital inertia tensors

$$\Theta_{aa}^J - B\Theta_{aa}^I = \frac{8\pi}{e^2} (\mathcal{I} - B^2) \int s_f^4 dr \geq 0, \quad \text{(A.16)}$$

because $\mathcal{I} \geq B^2$. The interference (mixed) inertia tensor, which also defines the isovector part of the magnetic transition operator, is equal to

$$\Theta_{ab}^{int} = \int s_f^2 \left\{ \left[\frac{F_\pi^2}{4} + \frac{1}{e^2} \left[(\partial_\nu f)^2 + s_f^2 (\partial_\nu \mathbf{n})^2 \right] \right] \times \\ \times \partial_i n_l - \frac{1}{e^2} (\partial_i f \partial_\nu f + s_f^2 \partial_i \mathbf{n} \partial_\nu \mathbf{n}) \partial_\nu n_l \right\} \times \\ \times n_k \epsilon_{kla} \epsilon_{i\alpha b} r_\alpha d^3 r. \quad \text{(A.17)}$$

The components of the spatial angular velocities interfere only with the components ω_1, ω_2, ω_3 of the angular rotation velocities in configuration space.

Numerically, the components of the mixed inertia tensor are much smaller than those of isotopical or orbital inertia tensor, except in special cases of «hedgehogs», where

$$\Theta^{int} = \Theta^I = \Theta^J,$$

and the axially symmetric configurations where the three-dimensional components of inertia satisfy the relations

$$\Theta_{33}^{int} = -n\Theta_{33}^I = -\Theta_{33}^J / n.$$

We finally note that the most general formulas for inertia tensors are presented here for the first time. For the RM configurations, they differ in some details from those given in the literature.

APPENDIX B

Electromagnetic transition operators

For completeness, we here prove some statements concerning the isovector (octet in the $SU(3)$ case) vector charge and the isovector magnetic moment operator in the general form.

The isovector current and the isospin generator are related by

$$V_{0,a} = \frac{1}{2}\operatorname{Tr}(A^\dagger\lambda_a A\lambda_b)I_b^{bf} = R_{ab}(A)I_b^{bf}, \quad (B.1)$$

where in the body-fixed coordinate system (connected with the soliton), the isospin generator is

$$I_b^{bf} = \frac{\partial L^{rot}(\omega,\Omega)}{\partial\omega_b}. \quad (B.2)$$

We have $a,b = 1,2,3$ for the $SU(2)$ model and $a,b = 1,\dots,8$ for the $SU(3)$ model. To prove this, we consider the ansatz

$$U = \exp(-i\alpha_a\lambda_a/2)A(t)U_0 A^\dagger(t)\exp(i\alpha_a\lambda_a/2). \quad (B.3)$$

The Noether vector current is the coefficient before the derivative of the probe function, $\partial_\mu\alpha$. In the lowest order in α, we obtain the chiral derivative

$$U^\dagger\partial_0 U = A\left[U_0^\dagger A^\dagger\times\right.$$
$$\left.\times\left(\dot A - \frac{i}{2}\dot\alpha A\right)U_0 - A^\dagger\left(\dot A - \frac{i}{2}\dot\alpha A\right)\right]A^\dagger. \quad (B.4)$$

Using the definition of the rotation angular velocities ω_a in configuration space, we obtain

$$A^\dagger\dot A - \frac{i}{2}A^\dagger\dot\alpha A = -\frac{i}{2}\lambda_b(\omega_b + R_{ab}(A)\dot\alpha_a), \quad (B.5)$$

where

$$R_{ab}(A) = \frac{1}{2}\operatorname{Tr}(A^\dagger\lambda_a A\lambda_b) \quad (B.6)$$

is a real orthogonal matrix. Because the dependence on $\dot\alpha$ reduces to a simple addition to angular velocity in accordance with (B.5), Eq. (B.1) follows immediately.

Because of the well known relation,

$$Q = B + \frac{I_3}{2} = B + \frac{V_{0,3}}{2}, \quad (B.7)$$

the baryonic (topological) charge and the third component of the isospin generator contribute to the charge of the quantized skyrmion.

We also prove that there is a simple relation between the isovector (octet for the $SU(3)$ model) magnetic momentum operator of the skyrmion and the

mixed (interference) inertia tensor. We first note that because of the Lorentz invariance, the Lagrangian of an arbitrary chiral model, not only the Skyrme model, can be presented as a linear combination of contributions of the form

$$\mathcal{L}_{M,N} =$$
$$= \operatorname{Tr}(U^\dagger\dot U M U^\dagger\dot U N - U^\dagger\partial_k U M U^\dagger\partial_k U N), \quad (B.8)$$

where M and N are some matrices. For example, $M = N = 1$ for the second-order term. The contribution of the first term in (B.8) to the rotational energy that is proportional to Ω and ω and therefore defines the mixed (interference) inertia tensor is (see (A.9))

$$\Theta_{ab}^{int}\omega_a\Omega_b = \int\operatorname{Tr}(U_0^\dagger A^\dagger\dot A U_0 - A^\dagger\dot A)\times$$
$$\times\tilde M U_0^\dagger\partial_k U_0\tilde N\dot r_k d^3r + \left(M\leftrightarrow N\right), \quad (B.9)$$

where $\tilde M = A^\dagger M A$ and $\tilde N = A^\dagger N A$. Thus,

$$\Theta_{ab}^{int} = -\frac{i}{2}\epsilon_{bjk}\int r_j(t)\operatorname{Tr}(U_0^\dagger\lambda_a U_0 - \lambda_a)\times$$
$$\times\tilde M U_0^\dagger\partial_k U_0\tilde N d^3r + \left(M\leftrightarrow N\right), \quad (B.10)$$

where $r_j(t)$ and ∂_k are body-fixed. From the second term in (B.8), we obtain the spatial components of the vector current,

$$V_k^a = \frac{i}{2}\operatorname{Tr}(U_0^\dagger A^\dagger\lambda_a A U_0 - A^\dagger\lambda_a A)\times$$
$$\times\tilde M U_0^\dagger\partial_k U_0\tilde N + \left(M\leftrightarrow N\right). \quad (B.11)$$

Recalling that

$$A^\dagger\lambda_a A = R_{ab}(A)\lambda_b, \quad R_{ab} = \frac{1}{2}\operatorname{Tr}A^\dagger\lambda_a A\lambda_b,$$

$$\partial_k = O_{lk}\partial_l^{bf},$$

we obtain

$$V_k^a = \frac{i}{2}R_{ab}O_{lk}\operatorname{Tr}(U_0^\dagger\lambda_b U_0 - \lambda_b)\times$$
$$\times\tilde M U_0^\dagger\partial_l U_0\tilde N + \left(M\leftrightarrow N\right). \quad (B.12)$$

By definition,

$$\mu_i^a = \frac{1}{2}\epsilon_{ijk}\int r_j V_k^a d^3r, \quad (B.13)$$

or

$$\mu_i^a = \frac{i}{4}\epsilon_{ijk}R_{ab}(A)O_{qk}O_{pj}\int r_p(t)\,\mathrm{Tr}(U_0^\dagger\lambda_b U_0-\lambda_b)\times$$
$$\times \tilde{M}U_0^\dagger\partial_q U_0\tilde{N} + \left(M\leftrightarrow N\right). \quad (B.14)$$

Because

$$\epsilon_{ijk}O_{pj}O_{qk} = \epsilon_{pql}O_{li},$$

we obtain the sought relation between components of the magnetic moment operator and the mixed inertia tensor in the body-fixed coordinate system:

$$\mu_i^a = -\frac{1}{2}R_{ab}(A)\Theta_{bl}^{int}O_{li}. \quad (B.15)$$

In some particular cases, this relation was used previously [8, 10].

To calculate the transition matrix elements, it is necessary to average this expression over wave functions of some initial and final states, see Sec. 2.

REFERENCES

1. T. H. R. Skyrme, Proc. Roy. Soc. A **260**, 127 (1961); Nucl. Phys. **31**, 556 (1962).

2. E. Witten, Nucl. Phys. B **223**, 433 (1983).

3. J. Gasser and H. Leutwyler, Nucl. Phys. B **250**, 465 (1985); U.-G. Meissner, COSY News, № 7, 6 (1999).

4. V. B. Kopeliovich and B. E. Stern, Pis'ma v ZhETF **45**, 165 (1987); NORDITA Preprint 89/34 (1989); J. J. M. Verbaarschot, Phys. Lett. B **195**, 235 (1987).

5. E. Braaten, S. Townsend, and L. Carson, Phys. Lett. B **235**, 147 (1990).

6. R. A. Battye and P. M. Sutcliffe, Phys. Rev. Lett. **79**, 363 (1997); ibid. **86**, 3989 (2001).

7. P. M. Sutcliffe, *Talk at the Int. Seminar Quarks-2000*, Pushkin, May 2000.

8. G. S. Adkins, C. R. Nappi and E. Witten, Nucl. Phys. B **228**, 552 (1983).

9. V. B. Kopeliovich, Yad. Fiz. **47**, 1495 (1988).

10. E. Braaten and L. Carson, Phys. Rev. D **38**, 3525 (1988).

11. L. Carson, Nucl. Phys. A **535**, 479 (1991); T. S. Walhout, Nucl. Phys. A **547**, 423 (1992); P. Irwin, Phys. Rev. D **61**, 114024 (2000).

12. G. Guadagnini, Nucl. Phys. B **236**, 35 (1984); A. P. Balachandran et al., Nucl. Phys. B **256**, 525 (1985); B. Schwesinger and H. Weigel, Phys. Lett. B **267**, 438 (1991); V. B. Kopeliovich, Phys. Lett. B **259**, 234 (1991); Yad. Fiz. **51**, 241 (1990); Nucl. Phys. A **547**, 315C (1992); C. L. Schat and N. N. Scoccola, Phys. Rev. D **62**, 074010 (2000).

13. V. B. Kopeliovich, Zh. Eksp. Teor. Fiz. **112**, 1941 (1997); Nucl. Phys. A **639**, 75C (1998); V. B. Kopeliovich, B. E. Stern, and W. J. Zakrzewski, Phys. Lett. B **492**, 39 (2000).

14. V. B. Kopeliovich, Yad. Fiz. **58**, 1317 (1995); ibid. **56**, 160 (1993).

15. C. Houghton, N. Manton, and P. Suttcliffe, Nucl. Phys. B **510**, 507 (1998).

16. R. A. Leese, N. S. Manton, and B. J. Schroers, Nucl. Phys. B **442**, 228 (1995).

17. B. Moussalam, Ann. of Phys. (N.Y.) **225**, 264 (1993).

18. H. Walliser, Phys. Lett. B **432**, 15 (1998); N. Scoccola and H. Walliser, E-print archive hep-ph/9805340; Phys. Rev. D **58**, 094037 (1998).

19. G. Holzwarth, Z. Physik A **356**, 339 (1996); Nucl. Phys. A **666**, 24 (2000).

20. L. D. Landau and E. M. Lifshitz, *Theoretical Physics, Vol. 3, Quantum Mechanics*, Nauka, Moscow (1974), §58, 110.

21. The DIB-2γ collaboration, JINR preprint E1-96-104 (1996); S. B. Gerasimov, E-print archives: nucl-th/9712064; nucl-th/9812077; A. S. Khrykin et al., E-print archives: nucl-ex/0012011; hep-ph/0101184.

22. H. Calen et al., Phys. Lett. B **427**, 248 (1998).

23. E. S. Konobeevsky, M. V. Mordovskoi, S. L. Potashev et al., Izv. Ross. Acad. Nauk **62**, 2171 (1998); L. V. Filkov, V. L. Kashevarov, E. S. Konobeevski et al., E-print archives: nucl-ex/9902002; hep-ex/9904003; Phys. Rev. C **61**, 044004 (2000).

24. V. B. Kopeliovich, B. Schwesinger, and B. E. Stern, Nucl. Phys. A **549**, 485 (1992).

25. I. R. Klebanov and K. M. Westerberg, Phys. Rev. D **53**, 2804 (1996); ibid. D **50**, 5834 (1994); V. B. Kopeliovich, Pis'ma v ZhETF **67**, 854 (1998); E-print archives hep-ph/9805296.

26. V. B. Kopeliovich and W. J. Zakrzewski, Pis'ma v ZhETF **69**, 675 (1999); Eur. Phys. J. C **18**, 369 (2000).

27. J. P. Garrahan, M. Schvellinger, and N. N. Scoccola, Phys. Rev. D **61**, 014001 (2000); C. L. Schat and N. N. Scoccola, Phys. Rev. D **61**, 034008 (2000).

28. J. Segar, M. Sripriya, and M. Sriram, Phys. Lett. B **342**, 201 (1995); V. B. Kopeliovich and M. S. Sriram, Yad. Fiz. **63**, 552 (2000).

29. B. F. Gibson, C. B. Dover, G. Bhamathi, and D. R. Lehman, Phys. Rev. C **27**, 2085 (1983).

30. J. T. Reed et al., Phys. Rev. **168**, 1495 (1968).

31. D. Grzonka and K. Kilian, Nucl. Phys. A **639**, 569C (1998); COSY-TOF collaboration, COSY News, № 4, 1 (1999).

32. J. K. Ahn et al., AIP Conf. Proc. **412**, 923 (1997); Nucl. Phys. A **639**, 379C (1998).

33. S. Kabana et al., J. Phys. G **23**, 2135 (1997).

34. T. Ioannidou, B. Piette, and W. J. Zakrzewski, J. Math. Phys. **40**, 6353 (1999); ibid. **40**, 6223 (1999).

35. Ya. B. Zeldovich, I. Yu. Kobzarev, and L. B. Okun, Zh. Eksp. Teor. Fiz. **67**, 3 (1974).

36. N. S. Manton and B. M. A. G. Piette, E-print archive hep-th/0008110.

37. V. B. Kopeliovich, Phys. Rept. **139**, 51 (1986).

38. T. Krupovnickas, E. Norvaisas, and D. O. Riska, E-print archive nucl-th/0011063.